On the effects of channel tortuosity on the close electromagnetic fields associated with lightning return strokes

J. Peer and A. Kendl

Institute for Ion Physics and Applied Physics,

University of Innsbruck, Technikerstr. 25, A-6020 Innsbruck, Austria

Abstract

The electromagnetic fields associated with tortuous lightning channels are usually characterised by a pronounced fine structure. This work investigates and quantifies the effects of channel tortuosity on the return stroke electromagnetic field shapes in the close lightning environment (the range up to 100 m from the lightning striking point). General equations for lightning return stroke electromagnetic fields for arbitrarily located observation points are derived from Maxwell's equations. In order to include arbitrary channel shapes, the channel is described by a parametric representation in Cartesian coordinates with the channel length as the free parameter. The return stroke current required for the evaluation of the derived equations is calculated from a current generation type model. The field computations show that amplitudes and waveforms of the electromagnetic fields in the close lightning environment are considerably influenced by the channel shape. In particular, the induction component of the electric fields radiated by a tortuous lightning channel differs significantly from that associated with a straight channel.

I. INTRODUCTION

In calculating the electromagnetic fields radiated by ground striking lightning discharges, the lightning channel is usually idealised by a straight and vertical line between cloud and ground. Due to the symmetry in such assumptions, the equations for the electric and magnetic fields can be formulated in cylindrical or spherical coordinates [e.g. 8–10, 12, 13].

The close electromagnetic fields associated with cloud-to-ground lightning, however, is characterised by a pronounced fine structure which is due to the tortuosity of the lightning channel. Recently, various approaches for the computation of electric and magnetic fields radiated by tortuous lightning channels have been published [e.g. 4, 7, 16]. The loss of radial symmetry in considering arbitrarily shaped channels necessitates the introduction of Cartesian coordinates which implicates an increase of complexity in deriving and solving the equations for the electromagnetic fields [16].

Section II of our work presents a detailed derivation of very general expressions for lightning return stroke fields. The equations are formulated in Cartesian coordinates and include both arbitrarily shaped lightning channels and arbitrarily located observation points. Moreover, a height variable return stroke velocity is taken into account. Arbitrary channel shapes are considered by the introduction of a parameter representation for the lightning channel with the channel length as the free parameter. Such a description allows the direct application of return stroke models which predict the current distribution as a function of the length coordinate of the lightning channel.

In our work, the return stroke current distribution required for the field computations is calculated on the basis of the current generation type model proposed by Cooray et al. [2]. The model includes the attachment process and enables thus to include the upward growing connecting leader. Moreover, it allows to take into account a height variable return stroke velocity. The model of Cooray et al. [2] and the modifications done in our work are briefly discussed in section III.

The equations derived in section II are evaluated for both a straight and a tortuous lightning channel. The tortuous channel used in the computations is formed from randomly generated parameters. The effects of channel tortuosity on the close electromagnetic fields are investigated in section III, too.

The presented computations were done within the framework of an investigation on the

action of lightning electromagnetic pulses on biological tissue. Biological tissue is mainly influenced by the electric fields which are induced by the transient magnetic pulses associated with return strokes. For this reason, a short paragraph of section III deals with the induced electric fields.

II. DERIVATION OF GENERAL EQUATIONS FOR LIGHTNING RETURN STROKE ELECTROMAGNETIC FIELDS

A. Geometry

The geometry used in deriving equations for the electric and magnetic fields radiated by a lightning return stroke is shown in figure 1. Cartesian coordinates with basis vectors $(\vec{\mathrm{e}}_x, \vec{\mathrm{e}}_y, \vec{\mathrm{e}}_z)$ are used. The lightning channel $\vec{l}(s) = l_x(s)\,\vec{\mathrm{e}}_x + l_y(s)\,\vec{\mathrm{e}}_y + l_z(s)\,\vec{\mathrm{e}}_z$ is parametrised by its length s, where s is measured from ground on upward. The base point of the channel is assumed to be the point of origin of the coordinate system. $R(s) = \sqrt{(\mathrm{d}\vec{l}(s) - \vec{r}) \cdot (\mathrm{d}\vec{l}(s) - \vec{r})}$ denotes the distance between a channel segment $\mathrm{d}\vec{l}(s)$ and the observation point $\vec{r} = x\,\vec{\mathrm{e}}_x + y\,\vec{\mathrm{e}}_y + z\,\vec{\mathrm{e}}_z$. The velocity distribution of the upward extending return stroke channel is assumed to be specified by a function $v(s)$. Real and retarded channel lengths at time t are denoted by $s = L(t)$ and $s = L_{\mathrm{ret}}(t)$, respectively.

B. Solution of Maxwell's equations for the current carrying return stroke channel

Maxwell's equations in vacuum are given by (since $\varepsilon_{\mathrm{r}} \approx 1$, $\mu_{\mathrm{r}} \approx 1$ in air, air can be idealised as vacuum)

$$\vec{\nabla} \cdot \vec{E}(\vec{r}, t) = \frac{\rho(\vec{r}, t)}{\varepsilon_0} \tag{1a}$$

$$\vec{\nabla} \cdot \vec{B}(\vec{r}, t) = 0 \tag{1b}$$

$$\vec{\nabla} \times \vec{E}(\vec{r}, t) = -\frac{\partial \vec{B}(\vec{r}, t)}{\partial t} \tag{1c}$$

$$\vec{\nabla} \times \vec{B}(\vec{r}, t) = \mu_0 \varepsilon_0 \frac{\partial \vec{E}(\vec{r}, t)}{\partial t} + \mu_0\, \vec{j}(\vec{r}, t) \tag{1d}$$

where $\vec{E}(\vec{r}, t)$ and $\vec{B}(\vec{r}, t)$ denote the electric field and the magnetic flux density, respectively. For the present case of a current carrying lightning channel parametrised by its length

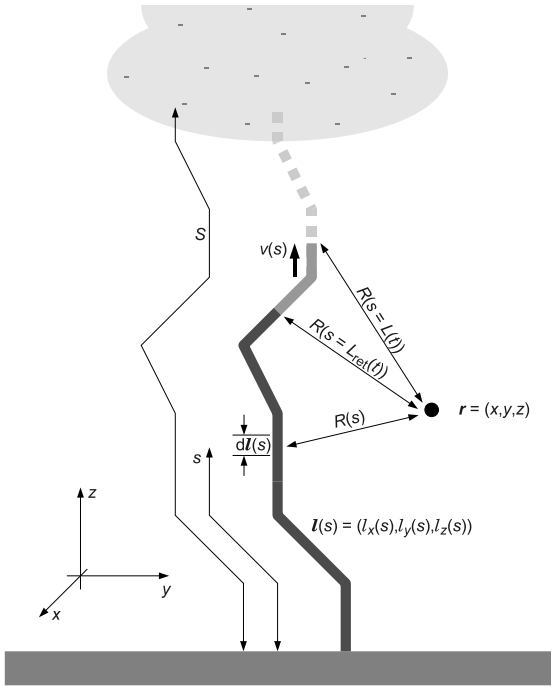

FIG. 1: *Geometry used in deriving equations for the electromagnetic fields radiated by a lightning return stroke. Real and retarded length of the lightning channel are illustrated by different shades of grey. The observation point is marked with $\vec{r}$. The grey bar indicates a perfectly conducting ground plane.*

coordinate, the current density $\vec{j}(\vec{r},t)$ can be expressed as

$$\vec{j}(\vec{r},t)\,\mathrm{d}^3r = i(s,t)\,\mathrm{d}\vec{l}(s) = i(s,t)\frac{\partial\vec{l}(s)}{\partial s}\,\mathrm{d}s \tag{2}$$

where $i(s,t)$ denotes the return stroke current distribution. There is no need to replace also the charge density $\rho(\vec{r},t)$. This is due to the fact that the scalar potential $\Phi(\vec{r},t)$ introduced by equation (3a) can directly be calculated from the Lorentz gauge (cf. eq. (4)). Equations (1) are solved by the introduction of the potentials $\Phi(\vec{r},t)$ and $\vec{A}(\vec{r},t)$ defined through

$$\vec{E}(\vec{r},t) = -\vec{\nabla}\Phi(\vec{r},t) - \frac{\partial\vec{A}(\vec{r},t)}{\partial t} \tag{3a}$$

$$\vec{B}(\vec{r},t) = \vec{\nabla}\times\vec{A}(\vec{r},t) \tag{3b}$$

Using the Lorentz gauge

$$\vec{\nabla}\cdot\vec{A}(\vec{r},t) = -\frac{1}{c^2}\frac{\partial\Phi(\vec{r},t)}{\partial t} \tag{4}$$

and combining equations (3) and (1), $\Phi(\vec{r},t)$ and $\vec{A}(\vec{r},t)$ can be expressed as

$$\Phi(\vec{r},t) = -\frac{1}{4\pi\varepsilon_0}\int_0^{L_{\rm ret}(t)}\int_{t_{\rm b}}^{t} \mathrm{d}s\,\mathrm{d}\tau\left[\vec{\nabla}\cdot\frac{i(s,t_{\rm ret}(s,\tau))}{R(s)}\,\frac{\partial\vec{l}(s)}{\partial s}\right] \tag{5a}$$

$$\vec{A}(\vec{r},t) = \frac{\mu_0}{4\pi}\int_0^{L_{\rm ret}(t)} \mathrm{d}s\left[\frac{i(s,t_{\rm ret}(s,t))}{R(s)}\,\frac{\partial\vec{l}(s)}{\partial s}\right] \tag{5b}$$

where $t_{\rm b} = |\vec{r}|/c$ denotes the time taken by a signal to propagate from the lightning striking point to the observation point $\vec{r}$, and $t_{\rm ret} = t - R(s)/c$ is the retarded time. Since retardation effects have to be taken into account, the s-integration is carried out along the retarded channel, that is, the range of integration is given by $[s=0, s=L_{\rm ret}(t)]$. Combining equations (3) and (5) yields

$$\begin{aligned} E_k(\vec{r},t) = \frac{1}{4\pi\varepsilon_0}\int_0^{L_{\rm ret}(t)} \mathrm{d}s\Bigg\{ & \\ \left[\sum_{j=x,y,z}\left(\frac{(r_j-l_j)(r_k-l_k)}{c^2R^3}\frac{\partial l_j}{\partial s}\right) - \frac{1}{c^2R}\frac{\partial l_k}{\partial s}\right]\frac{\mathrm{d}}{\mathrm{d}t}i(s,t_{\rm ret}) & \\ + \sum_{j=x,y,z}\left(\frac{3(r_j-l_j)(r_k-l_k) - R^2\,\delta_{jk}}{cR^4}\frac{\partial l_j}{\partial s}\right) i(s,t_{\rm ret}) & \\ + \sum_{j=x,y,z}\left(\frac{3(r_j-l_j)(r_k-l_k) - R^2\,\delta_{jk}}{R^5}\frac{\partial l_j}{\partial s}\right)\int_{t_b}^{t}\mathrm{d}\tau\, i(s,t_{\rm ret}\Bigg\} & \end{aligned} \tag{6a}$$

$$\begin{aligned} B_k(\vec{r},t) = \frac{\mu_0}{4\pi}\int_0^{L_{\rm ret}(t)} \mathrm{d}s\Bigg[& \left(\frac{1}{R^3}i(s,t_{\rm ret}) + \frac{1}{cR^2}\frac{\mathrm{d}}{\mathrm{d}t}i(s,t_{\rm ret})\right) \\ & \sum_{l,m=x,y,z}(l_l - r_l)\frac{\partial l_m}{\partial s}\varepsilon_{klm}\Bigg] \end{aligned} \tag{6b}$$

where the Levi-Civita symbol ε_{klm} is given by

$$\varepsilon_{klm} = \begin{cases} 1 & \text{if} \quad (k,l,m) = (x,y,z),(y,z,x),(z,x,y) \\ -1 & \text{if} \quad (k,l,m) = (z,y,x),(y,x,z),(x,z,y) \\ 0 & \text{otherwise} \end{cases} \tag{7}$$

For the sake of a better oversight the $\vec{r}$-, s-, and t-dependences of $\vec{l}(s)$, $R(s)$, and $t_{\rm ret}(\vec{r},t)$ are omitted in equations (6).

Details to the presented solution method of Maxwell's equations can be found in many textbooks [e.g. 15].

Similar equations for lightning electromagnetic fields are presented in several publications, most of them based on the assumptions of a straight and vertical lightning channel and an observation point on ground (i.e. $z = 0$) [e.g. 8–10, 12, 13].

Zhao and Zhang [16] derived equations for the electromagnetic fields radiated by arbitrarily shaped lightning channels. Their approach is very similar to that used in our work. In contrast to our work, however, their equations do not consider arbitrarily located observation points.

Equations (6) are thus the most general expressions for lightning return stroke fields and include all other formulations as special cases. Assuming a straight and vertical lightning channel (i.e. $\vec{l}(s) = s\,\vec{e}_z$) and an observation point on ground (i.e. $z = 0$), for example, equations (6) pass into those usually presented in the literature [e.g. 5, 10, 12]. On the other hand, equations (6) correspond to the equations presented by Zhao and Zhang [16] if an observation point on ground (i.e. $z = 0$) is assumed.

It should be mentioned that equations (6) do not include effects arising from a conducting ground plane (cf. subsec. II C).

C. The presence of a conducting ground plane

The presence of earth's surface is not yet included in equations (6). Usually, the ground plane is taken into account by considering an image channel carrying a current of opposite polarity and direction [e.g. 13]. The fields at a given observation point then consist of the contributions from the real and the image channel. For an observer on a perfectly conducting ground plane the contributions of real and image channel are of equal magnitude, so that the vertical electric field and the horizontal magnetic flux density are given by the double of E_z, B_x, and B_y from equations (6). The horizontal electric field and the vertical magnetic flux density vanish on the surface of a perfect conductor. When considering observation points above ground, the contributions of real and image channel have to be calculated separately.

D. Real and retarded channel lengths for an extending lightning channel

In order to calculate the real and retarded channel lengths for a return stroke channel extending with velocity $v(s)$, the average velocity of the return stroke front between ground and length coordinate s is introduced [11]

$$v_{\mathrm{av}}(s) = \frac{s}{t_{\mathrm{u}}(s)} = \frac{s}{\int\limits_0^s \frac{\mathrm{d}\sigma}{v(\sigma)}} \tag{8}$$

$t_{\mathrm{u}}(s)$ denotes the time taken by the return stroke front to propagate from ground to s. The time depending real length $L(t)$ can be calculated by solving the equation

$$t_{\mathrm{u}}(L) = \int\limits_0^{s=L} \frac{\mathrm{d}\sigma}{v(\sigma)} = t \tag{9}$$

Considering retardation effects, that is, taking into account that a given time t comprises the time taken by the return stroke front to reach the retarded length $L_{\mathrm{ret}}(t)$ and the time taken by the signal to propagate to the observation point, the retarded channel length can be calculated from [cf. 11]

$$t = \frac{L_{\mathrm{ret}}(t)}{v_{\mathrm{av}}(L_{\mathrm{ret}}(t))} + \frac{R(L_{\mathrm{ret}}(t))}{c} \tag{10}$$

For observation points above ground the same calculation must be done for the image channel, too.

III. COMPUTATION OF THE CLOSE ELECTROMAGNETIC FIELDS RADIATED BY STRAIGHT AND TORTUOUS RETURN STROKE CHANNELS

A. Return stroke model

Equations (6) were evaluated for a current generation type model of the return stroke. The model of Cooray et al. [2], which refers to first return strokes and includes the attachment process, that is, the preceding upward growing connecting leader, was modified in order to describe subsequent return strokes, too. For this purpose, the channel base current used by Cooray et al. [2] was replaced by a current waveform typical for subsequent return strokes. Moreover, the length of the upward growing connecting leader, which Cooray et al. [2] calculated by estimating the potential difference in the gap between connecting and

dart leader, was replaced by a typical experimental value. In simple terms, the required model input parameters are the channel base current, the leader charge distribution, and the velocity distribution of both connecting leader and subsequent return stroke. Details can be found in Cooray et al. [2].

Within the framework of our field computations we investigated also the electromagnetic fields radiated by first return strokes. Cooray et al. [2] showed that the close electromagnetic fields associated with first return strokes strongly depend on the assumed velocity distribution of the return stroke front. The influence of the velocity distribution on the electromagnetic fields radiated by subsequent return strokes was not explicitly investigated in our work. From a physical point of view, however, the upward growing connecting leader can be assumed to have a considerable influence on the close electromagnetic fields, even though the connecting leader is comparatively unpronounced for subsequent return strokes.

The channel base current used in our computations is shown in figure 2. It consists of the sum of two Heidler functions [cf. 5] with a parameter set introduced by Diendorfer and Uman [3]. The leader charge distribution was assumed to take the constant value of $0.14\,\mathrm{mC\,m^{-1}}$. The length of the connecting leader was set to 10 m. These experimental values were taken from Rakov and Uman [6]. The calculated velocity distribution is shown in figure 3.

The return stroke model was implemented in Matlab 7.6 (The MathWorks Inc., Natick, US-MA). The analytical formulation and the numerical methods in solving the appearing integral equation for the channel current were adapted from Thottappillil and Uman [11] and Cooray [1]. The computed return stroke current distribution is shown in figure 2.

B. Tortuous lightning channel

The tortuous lightning channel used in our field computations was formed by a series of straight segments. The lengths of the single segments were generated randomly from a Gaussian distribution with a mean value of 20 m and a standard deviation of 10 m. The inclination angle of each segment, that is, the angle between the segment and the z-axis, was taken from a Gaussian distribution with a mean value of 16° and a standard deviation of 11.5°. The azimuth was assumed to be uniformly distributed between 0° and 360° . These parameters were chosen on the basis of those used by Lupo et al. [4] and Vargas and Torres [14]. The resulting tortuous channel is shown in figure 4.

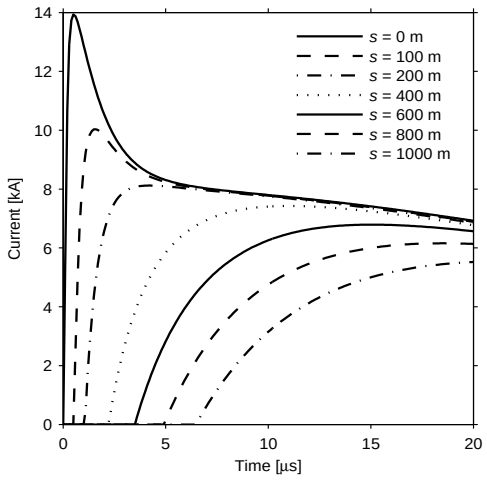

FIG. 2: *Return stroke current at different length coordinates in the lightning channel. The waveform associated with* $s = 0\,\mathrm{m}$ *corresponds to the assumed channel base current.*

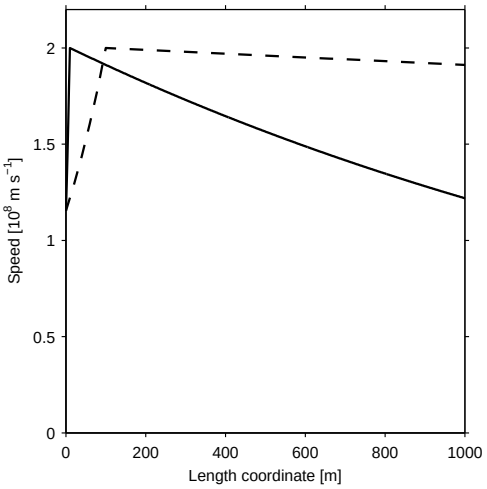

FIG. 3: *Return stroke velocity distribution as a function of the length coordinate* s*. The dashed line shows the velocity on a ten times faster length scale where the portion of the upward growing connecting leader becomes visible.*

C. Radiated electromagnetic fields

Return stroke electromagnetic fields were computed for both a straight and vertical, and a tortuous channel. In the following discussion the indices "tort" and "str" refer to the fields associated with the tortuous and the straight lightning channel, respectively.

The results for the electric fields and the magnetic flux densities are shown in figures 5 and

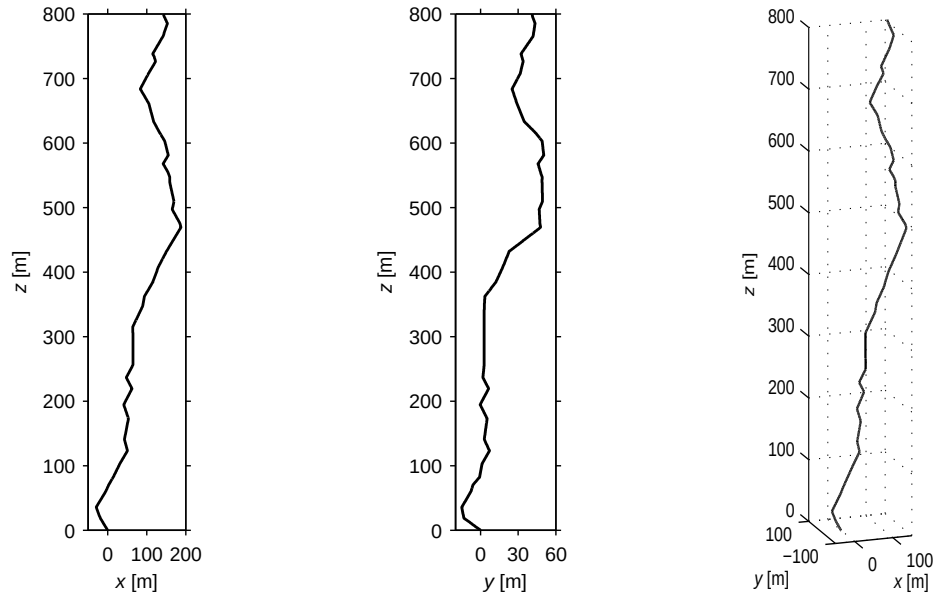

FIG. 4: *2D and 3D perspectives of the tortuous lightning channel used for the field computations. The tortuosity was randomly generated. Note that the lowest channel sections (roughly the first 50 m) are inclined away from an observer on the positive x-axis and inclined toward an observer on the negative x-axis.*

6. The observation points were assumed to be on ground along the x-axis, that is, $|x|$ gives the distance from the lightning striking point. While for the straight and vertical lightning channel the magnetic flux density in x-direction vanishes due to the radial symmetry, the tortuous channel radiates small magnetic fields in x-direction, too. Due to the assumption of a perfectly conducting ground plane, the horizontal electric fields vanish for both channels.

According to figures 5 and 6, the fields associated with the straight and the tortuous channel mainly differ in the maximum amplitudes. Moreover, the fields radiated by the tortuous channel show an additional fine structure which changes the waveforms of the radiated electromagnetic fields. In the following paragraphs these properties are discussed in more detail.

Zhao and Zhang [16] presented a similar discussion of the electromagnetic fields radiated by tortuous return stroke channels. They investigated the azimuthal dependency of the remote fields ($100\,\mathrm{m} - 100\,\mathrm{km}$ from the lightning striking point). Our work, on the contrary, concentrates on the radial dependency of the very close return stroke fields ($20 - 100\,\mathrm{m}$ from the lightning striking point). Thus, it can be regarded as a supplement to the discussion of

Zhao and Zhang [16].

1. *Electric fields*

In the limit $t \to \infty$ the close electric fields shown in figure 5 converge to a constant value. This means that they are mainly electrostatic, that is, they are dominated by the electrostatic part of equation (6a) (i.e. the fourth line in eq. (6a)), which is the only part providing a finite contribution for $t \to \infty$. Note that the electrostatic part is proportional to R^{-5}, while the other parts of equation (6a) are proportional to R^{-4} and R^{-3}, respectively. Thus, the electrostatic part mainly contributes to the close electric fields.

The maximum amplitudes of the radiated electric fields considerably depend on the observation point (cf. fig. 5). At $x = 20\,\mathrm{m}$, for example, the maximum amplitude of E_{tort} reaches only 52 % of the value associated with E_{str}. At $x = -20\,\mathrm{m}$, on the other hand, the maximum amplitude of E_{tort} is 1.xxx times larger than that of E_{str}. Both, the increase of E_{tort} for observation points along the positive x-axis and the decrease of E_{tort} for observation points along the negative x-axis are due to the shape of the tortuous lightning channel: The lowest sections (i.e. the first 50 m) of the sample channel shown in figure 4 are inclined toward an observation point along the positive x-axis and inclined away from an observation point on the negative x-axis. After the first 50 m the channel inclination is reversed. This is reflected in the electric fields at $x = 100\,\mathrm{m}$, where the E_{tort} is larger than E_{str}. The close electromagnetic fields radiated by tortuous lightning channels thus strongly depend on the orientation of those channel segments which primarily contribute to the total fields a given observation point.

2. *Magnetic fields*

The orientation of the lowest channel segments is reflected in the magnetic fields, too (cf. fig. 6). At $x = 20\,\mathrm{m}$, the maximum value of B_{tort} reaches roughly 70 % of the value associated with B_{str}. At $x = 20\,\mathrm{m}$, on the other hand, the peak value of B_{tort} is more than 1.5 times larger than the peak value of B_{str}. Since the assumed tortuous channel is "quite" straight, the main portion ($\sim 85\,\%$) of the magnetic fields is radiated in y-direction (cf. fig. 6(b), fig. 6(c), and fig. 6(d), fig. 6(e)).

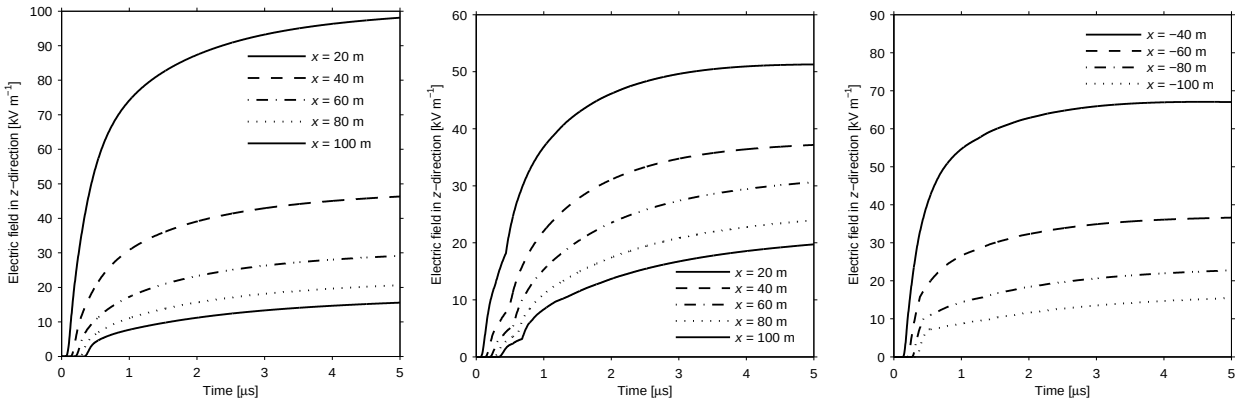

(a) (b) (c)

FIG. 5: *Computed return stroke electric fields for a straight (a) and a tortuous (b) lightning channel. The observer was assumed to be located on different positions along the x-axis. Due to the assumption of a perfectly conducting ground plane, the horizontal electric fields vanish.*

The magnetic fields associated with the tortuous channel show a pronounced fine structure. The relative amplitudes of the additional maxima are observed to increase with increasing distance from the lightning striking point (most clearly visible in fig. 6(c)). This simply reflects the fact that the very close magnetic fields are mainly dominated by the lowest channel segments, while with increasing distance also the higher channel sections contribute.

The peak values of B_{tort} are furthermore observed to be shifted with respect to the peak values of B_{str} (cf. fig. 6(a), fig. 6(b), fig. 6(d)). At $x = 20\,\mathrm{m}$ the peak value of B_{tort} is reached $0.3\,\mu\mathrm{s}$ later than that of B_{str}. At $x = -20\,\mathrm{m}$ it is reached $0.3\,\mu\mathrm{s}$ earlier. The magnitude of this shift is observed to decrease with increasing distance. This suggests the shift to be due to the orientation of those channel sections which mainly contribute to the fields at a given observation point. Generally, a shift of the peak values implicates that B_{tort} increases faster or more slowly than B_{str}. If the channel sections contributing to the fields at a given observation point are inclined away from the observer, the fields are characterised by a more flat increase. Channel sections inclined towards the observer, on the other hand, result in a steeper increase. The channel orientation thus considerably effects the time derivative of the magnetic fields. This in turn has a strong influence on the induction component of the electric fields, that is, the electric fields induced by the transient magnetic pulses. The effect of channel tortuosity on the induced electric fields is discussed in subsection III C 3.

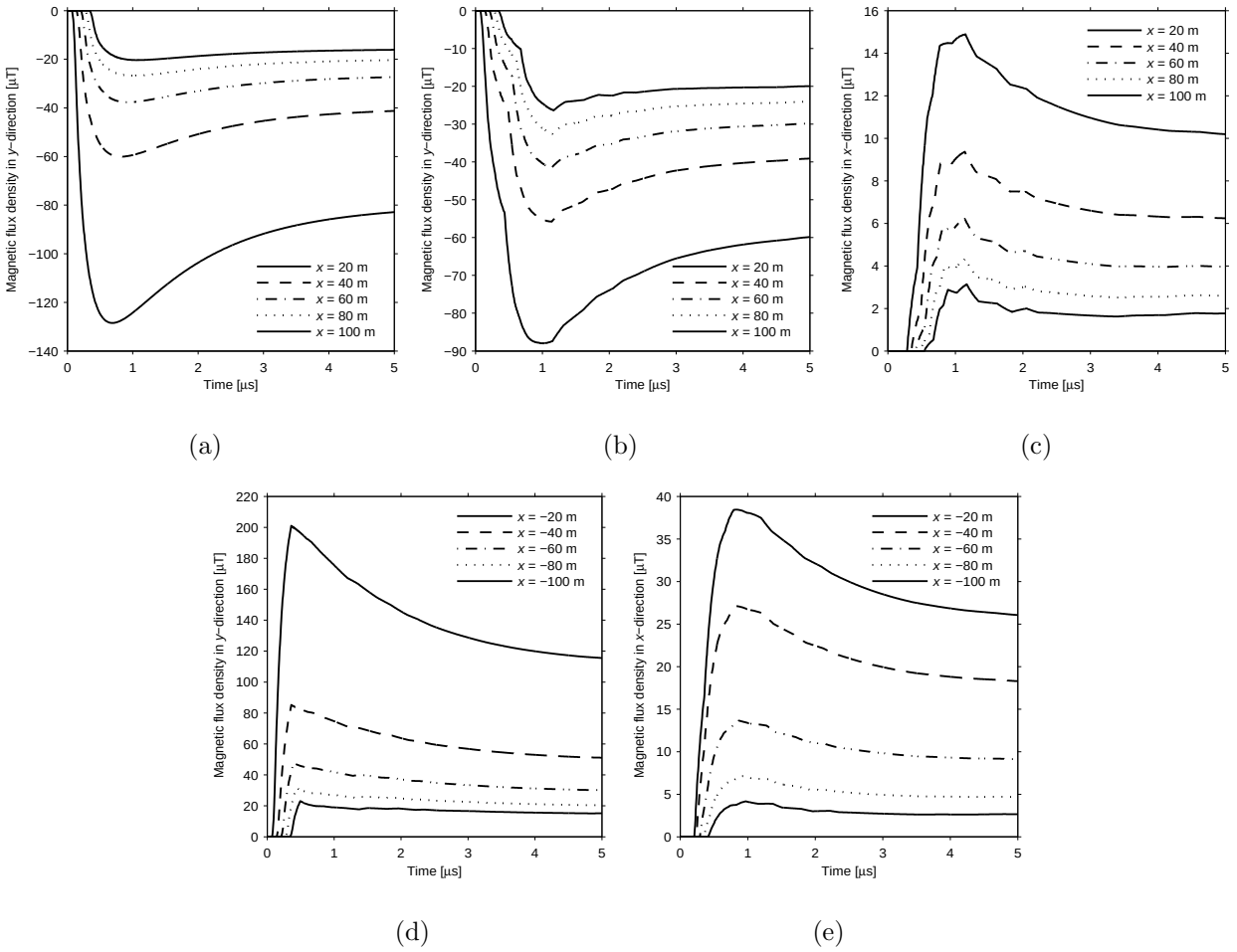

FIG. 6: *Computed return stroke magnetic flux densities for a straight (a) and a tortuous (b, c, d, e) lightning channel. The observer was assumed to be located on different positions along the x-axis. The vertical magnetic flux densities of real and image channel cancel on a perfectly conducting ground plane.*

3. Induced electric fields

The results of the field computations presented in the paragraphs III C 1 and III C 2 were used for an investigation on the action of return stroke magnetic pulses on biological tissue. Without going into detail it should be mentioned that the action of magnetic fields on biological tissue mainly happens by the electric fields which are induced by transient magnetic pulses. This paragraph presents a short discussion on the effects of channel tortuosity on the induced electric fields.

The induced electric fields, in the following labelled with E^{ind}, are given by the first

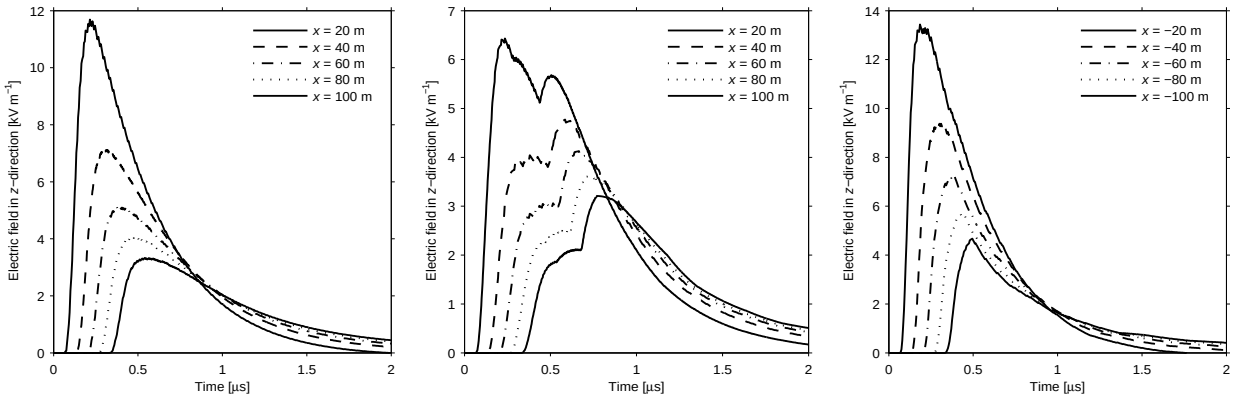

(a) (b) (c)

FIG. 7: *Computed induced return stroke electric fields for a straight (a) and a tortuous (b, c) lightning channel. The observer was assumed to be located on different positions along the x-axis. Due to the assumption of a perfectly conducting ground plane, the horizontal induced electric fields vanish.*

term of equation (3a). Figure 7 shows the results of a numerical evaluation of this term. A comparison of figures 7(a), 7(b), and 7(c) makes clear that the shape of the lightning channel strongly influences the induced electric fields. At $x = 20\,\mathrm{m}$ the peak value of $E^{\mathrm{ind}}_{\mathrm{tort}}$ reaches only 55 % of the corresponding value of $E^{\mathrm{ind}}_{\mathrm{str}}$. At $x = -20\,\mathrm{m}$, on the other hand, the peak value of $E^{\mathrm{ind}}_{\mathrm{tort}}$ is more than 1.1 % higher than that of $E^{\mathrm{ind}}_{\mathrm{str}}$. It is furthermore observed that the fields associated with straight and tortuous channels mainly differ in the peak range, while their shapes are similar in the initial fast increase and the final slow decrease.

The induced electric fields reflect the properties of the magnetic fields discussed in subsection III C 2. The magnetic fields associated with the tortuous channel were found to increase faster or more slowly than those associated with the straight channel (remember the shifts of the maxima of B_{tort}). Since the amplitudes of the induced electric fields depend on the time derivative of the magnetic fields (cf. eq. (1c)), this explains the fact that the induced electric fields are larger for observation points along the positive x-axis, and smaller for observation points along the negative x-axis. The main changes in the induced electric fields are due to the fastest changes in the magnetic fields. Therefore, the main changes of the induced electric fields concentrate on the first two microseconds. The peak value in the induced electric fields corresponds to the point in time with the largest changes in the magnetic fields (cf. fig. 6, fig. 7).

For the sake of completeness it should be mentioned that the induced electric fields are of course included in the total electric fields shown in figure 5. In the close lightning environment, however, they are superimposed by the electrostatic component and thus not explicitly visible.

D. Computational methods

Equations (6) were implemented in Matlab 7.6 (The MathWorks Inc., Natick, US-MA). In carrying out the numerical integrations the trapezoidal rule was used. For the field integrations a total channel length S (cf. fig. 1) of 1000 m was assumed, which is enough when the fields on ground within 100 m from the lightning striking point are considered. Time and length steps were set to $5 \cdot 10^{-9}$ s and 1 m, respectively. For the fields at distances of 20 m and 40 m partly also higher resolutions were needed.

IV. SUMMARY AND CONCLUSIONS

Very general equations for lightning electric and magnetic fields including both arbitrarily shaped lightning channels and arbitrarily located observation points were derived from Maxwell's equations. The lightning channel was described by a parametric representation in Cartesian coordinates. Equations for the determination of real and retarded channel lengths for the case of a height variable return stroke speed were presented. In order to discuss the effect of channel tortuosity on the close return stroke electromagnetic fields, the derived equations were solved for a current generation type model of the lightning return stroke. Return stroke electromagnetic fields were computed for both a straight and vertical, and a randomly generated tortuous lightning channel. Moreover, the electric fields induced by the transient return stroke magnetic pulses were investigated.

The results show that the global amplitudes of the close electromagnetic fields radiated by a tortuous lightning channel mainly depend on the orientation of the lowest channel sections. The relative amplitudes of the additional fine structure due to the channel tortuosity are observed to increase with increasing distance from the striking point, which was reduced to the fact that with increasing distance more different orientated channel sections contribute to the fields at a given observation point. Furthermore, the maximum of the magnetic

fields radiated by tortuous lightning channels was found to be shifted with respect to the magnetic fields associated with a straight channel. The shift implicates a change in the time derivative of the magnetic fields radiated by tortuous channels. This in turn was found to have a remarkable influence on amplitudes and waveforms of the induced electric fields.

---

[1] V Cooray. Predicting the spatial and temporal variation of the electromagnetic fields, currents, and speeds of subsequent return strokes. *IEEE Trans. Electromagn. Compat.*, 40:427–435, 1998.

[2] V Cooray, R Montano, and V Rakov. A model to represent negative and positive lightning first strokes with connecting leaders. *J. Electrost.*, 60:97–109, 2004.

[3] G Diendorfer and MA Uman. An improved return stroke model with specified channel-base current. *J. Geophys. Res.-Atmos.*, 95:13621–13644, 1990.

[4] G Lupo, C Petrarca, V Tucci, and M Vitelli. EM fields associated with lightning channels: On the effect of tortuosity and branching. *IEEE Trans. Electromagn. Compat.*, 42:394–404, 2000.

[5] VA Rakov and MA Uman. Review and evaluation of lightning return stroke models including some aspects of their application. *IEEE Trans. Electromag. Compat.*, 40:403–426, 1998.

[6] VA Rakov and MA Uman. *Lightning: Physics and effects*. Camb. Univ. Press, 2006.

[7] TX Song, YH Liu, and JM Xiong. Computations of electromagnetic fields radiated from complex lightning channels. *Prog. Electromagn. Res.-Pier*, 73:93–105, 2007.

[8] R Thottappillil and VA Rakov. On different approaches to calculating lightning electric fields. *J. Geophys. Res.-Atmos.*, 106:14191–14205, 2001.

[9] R Thottappillil, VA Rakov, and N Theethayi. Expressions for far electric fields produced at an arbitrary altitude by lightning return strokes. *J. Geophys. Res.-Atmos.*, 112:D16102, 2007.

[10] R Thottappillil, VA Rakov, and MA Uman. Distribution of charge along the lightning channel: Relation to remote electric and magnetic fields and to return-stroke models. *J. Geophys. Res.-Atmos.*, 102:6987–7006, 1997.

[11] R Thottappillil and MA Uman. Lightning return stroke model with height-variable discharge time constant. *J. Geophys. Res.-Atmos.*, 99:22773–22780, 1994.

[12] R Thottappillil, MA Uman, and VA Rakov. Treatment of retardation effects in calculating

the radiated electromagnetic fields from the lightning discharge. *J. Geophys. Res.-Atmos.*, 103:9003–9013, 1998.

[13] R Thottappillil, MA Uman, and N Theethayi. Electric and magnetic fields from a semi-infinite antenna above a conducting plane. *J. Electrost.*, 61:209–221, 2004.

[14] M Vargas and H Torres. On the development of a lightning leader model for tortuous or branched channels - Part I: Model description. *J. Electrost.*, 66:482–488, 2008.

[15] A Wachter and H Hoeber. *Compendium of theoretical physics*. Springer Sci. Bus. Media Inc., 2005.

[16] ZK Zhao and QL Zhang. Influence of channel tortuosity on the lightning return stroke electromagnetic field in the time domain. *Atmos. Res.*, 91:404–409, 2009.